Bollettino di Geofisica Teorica ed Applicata Vol. 56, n. 3, pp. 367-382; September 2015
DOI 10.4430/bgta0153

Fault population recognition through microseismicity in Mygdonia region (northern Greece)

C. Gkarlaouni[1], E. Papadimitriou[1], V. Karakostas[1], A. Kilias[2] and S. Lasocki[3]

[1] *Geophysics Department, School of Geology, Aristotle University, Thessaloniki, Greece*
[2] *Geology Department, School of Geology, Aristotle University, Thessaloniki, Greece*
[3] *Institute of Geophysics, Polish Academy of Sciences, Warsaw, Poland*

(Received: September 17, 2014; accepted: February 27, 2015)

ABSTRACT Seismicity in the area of Mygdonia basin (northern Greece) is lately characterized by a lack of strong events ($M \geq 5.0$) on the seismogenic faults known to have been repeatedly activated in the past. Only small to moderate magnitude earthquakes ($M \leq 4.8$) have occurred since 2000 in the area. Therefore, microseismicity is the only available information to be exploited for the identification of active faults and hazard assessment, since it may occur everywhere, as well as onto the major hazardous faults. Earthquakes recorded between 2000 and 2014 by the Hellenic Seismological Network were relocated by using the available P- and S-seismic wave arrivals in order to improve location accuracy. The V_P/V_S velocity ratio which was found equal to 1.78, along with station time delays, were all included in the Hypoinverse computer program. In the case of strong spatial or temporal clustering the HypoDD algorithm was employed for further improving location accuracy. The relocated seismicity was used to outline the geometrical properties of the local fault population and identify seismogenic faults deprived of a clear surface expression. Cross-sections made perpendicular to the main axis of the seismicity alignments, shed more light to the local fault network.

Key words: microseismicity, relocation, Wadati, Mygdonia graben.

1. Introduction

Investigation of minor earthquakes ($M \leq 4.0$) can provide insight to seismicity processes or seismic sources of large earthquakes before they occur. Small events are usually related to the same seismogenic processes as the fault population of larger earthquakes. Moderate ($M \approx 4.0$-5.5) and small earthquakes ($M < 4.0$) are related to main or subsidiary faults, which, along with the main rupture zones, supplement the fault populations in active seismotectonic areas. The importance of acquiring precisely defined focal parameters of microseismicity is based upon the fact that when strong events are lacking, minor earthquakes is the only source of information when seeking for faulting and seismogenesis patterns (Bagh *et al.*, 2007; Maggi *et al.*, 2009; Tan, 2012). Microseismicity engagement for this purpose is encouraged by the deployment of a dense and modern seismological network, which significantly contributed to lower magnitude

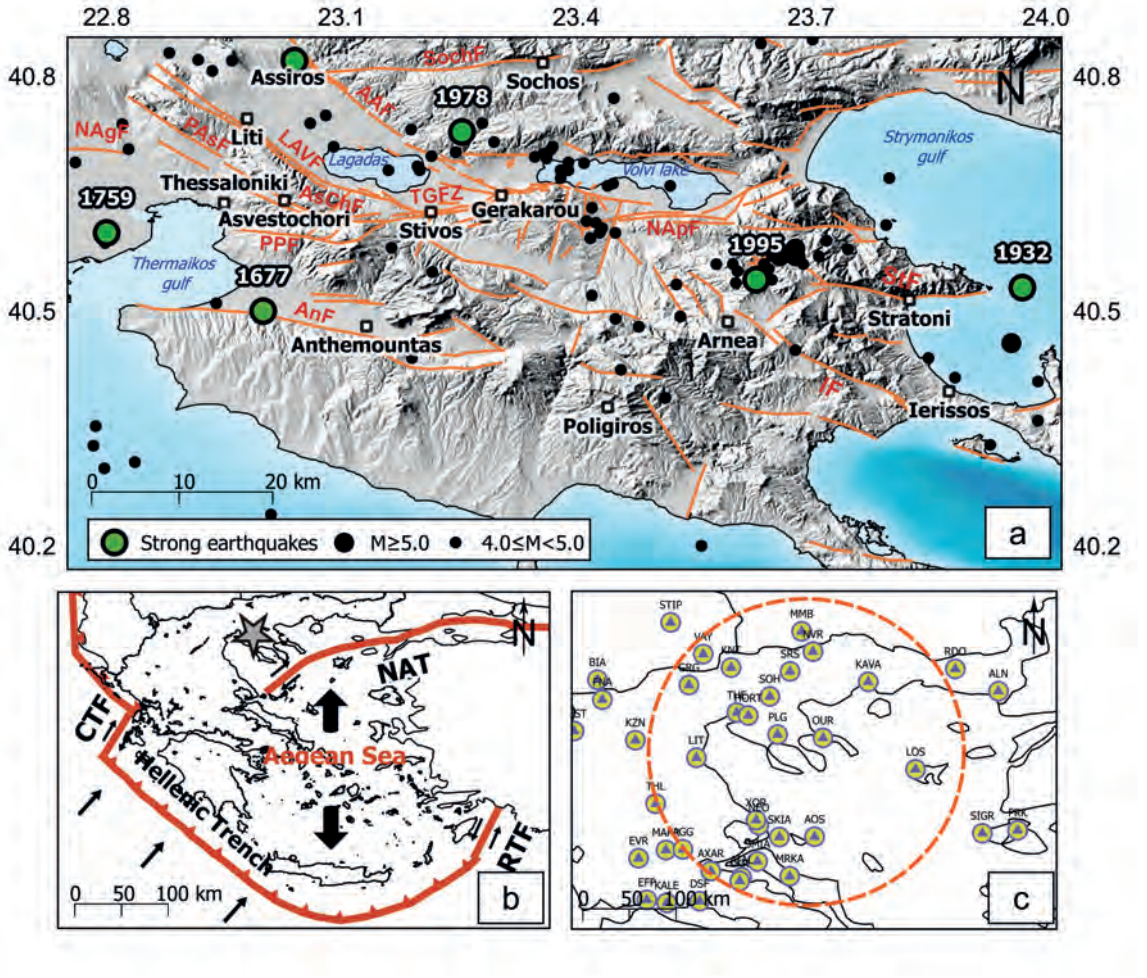

Fig. 1 - a) Digital elevation model for Mygdonia basin. Red lines correspond to important rupture zones, such as the E-W Thessaloniki-Gerakarou (TGFZ) normal fault zone, along with secondary fault segments described in the text (fault information gathered by Pavlides and Kilias, 1987; Tranos *et al*., 2003; Mountrakis *et al*., 2006). Green circles denote strong earthquakes (M≥6.5) and black dots depict earthquake epicentres with M≥4.0 since 1981. b) Simplified map of the broader Aegean Sea with the dominant seismotectonic features. The asterisk denotes the location of the study area, while arrows indicate the dominant plate kinematics. c) Map of northern Greece with the installed seismological stations belonging to the HUSN. The red circle encloses seismological stations employed for data re-processing using Wadati methodology and the calculation of station time delays.

detectability and recording. Although data provision was enhanced and location accuracy was improved, a number of uncertainties, inevitably involved in the existing earthquake catalogue, necessitates relocation for finer seismicity to be revealed. Therefore, the challenge of the present study is the recognition of the seismic sources evidenced by accurately located local seismicity for the Mygdonian area (northern Greece; Fig. 1a). Our study area comprises a neotectonic graben situated in the back-arc Aegean Sea, where a number of devastating earthquakes have occurred. The seismotectonic properties of the broader Aegean microplate are attributed to the subduction and the retreat of the Mediterranean oceanic microplate under the fast southward moving Aegean, giving rise to the Hellenic Arc (Papazachos and Comninakis, 1971; McKenzie, 1978).

The main seismotectonic features of the Aegean (Fig. 1b) are the Hellenic Trench (thick red line with triangles), the North Aegean Trough (NAT) which accommodates the westward extrusion of the Anatolian plate into the Aegean, the Cephalonia transform fault (CTF) and the Rodos operating transform fault (RTF). In the past, a number of strong events with maximum macroseismic intensities equal to IX (1759 Anthemountas earthquake; 1902 Assiros earthquake) and X (1932 Ierissos earthquake) have occurred in the study area [Papazachos and Papazachou, 2003 (Fig 1a)]. However, the current seismotectonic pattern is described by low seismicity rate and sparse moderate magnitude events. However, the existing seismic sources are still posing a potential societal threat for the city of Thessaloniki and the surrounding urban areas. The determination of the active fault segments responsible for the recent seismicity in this back-arc tectonic basin as well as the variations of seismicity clustering in time and space were the motivations of this study.

2. Seismotectonic framework

Mygdonia graben comprises a dense fault network that largely accommodates extensional tectonic processes, developed in the fast deforming back-arc Aegean area. The present form of the S-shaped Mygdonia basin comprises the impact of successive seismotectonic events, associated with extensional deformation and subsequent rotations of the stress field (Pavlides and Kilias, 1987). As a result, a complicated faulting network that incorporates NW-SE, NE-SW, E-W and NNE-SSW faults was formed, built on pre-existing structures. Most of these structures are strongly imprinted upon the relief and define the geomorphological barriers of the main or smaller elongated basins.

The active faults which are verified by seismotectonic observations to be associated with seismic activity are mainly developed in an E-W direction, controlling the central part of the basin and the eastern part of Chalkidiki Peninsula (Tranos *et al.*, 2003; Mountrakis *et al.*, 2006). The predominant feature is the E-W trending Thessaloniki-Gerakarou fault zone (TGFZ) and the semi parallel fault branches of Pilea-Peristera (PPF), Pefka-Asvestochori (PAsF) and Asvestochori-Chortiatis (AChF) fault segments (Fig. 1a). The prolongation of TGFZ zone to the east is composed of Nea Apollonia fault zone (NApF) along with subsidiary antithetic or sub parallel faults in between the two lakes or to the north of Volvi Lake. Sochos fault (SochF) corresponds to an impressive rupture zone along the northern margin of the basin steeply south-dipping and easily detected in aerial imagery. Anthemountas detachment fault (AnF) and Stratoni fault zone (StF) do not currently exhibit significant activity, however they are considered to be the causative sources for strong historical earthquakes. The NW-SE aligned fault zones follow inherited structures and they mainly consist of the north dipping Lagina-Agios Vasileios fault (LAvF) and the antithetic Assiros-Analipsi fault system (AAF) as well as Ierissos fault zone (IF) which also plays an important role in the evolution of the study region.

After the 1978 Stivos strong earthquake (M=6.5) and its stronger aftershocks (M=5.3 and M=5.8), seismicity rate is reduced, with the absence of strong events ($M\geq$6.0) interrupting normal seismicity. In May 1995, the Arnea seismic sequence occurred at the mountainous area of Chalikidiki Peninsula, where two earthquakes with magnitudes M=5.0 and M=5.1, preceded the strongest event (M=5.3). Considerable seismological research has been conducted for this area with most of the studies referring to the 1978 strong seismic triplet (Papazachos *et al.*,

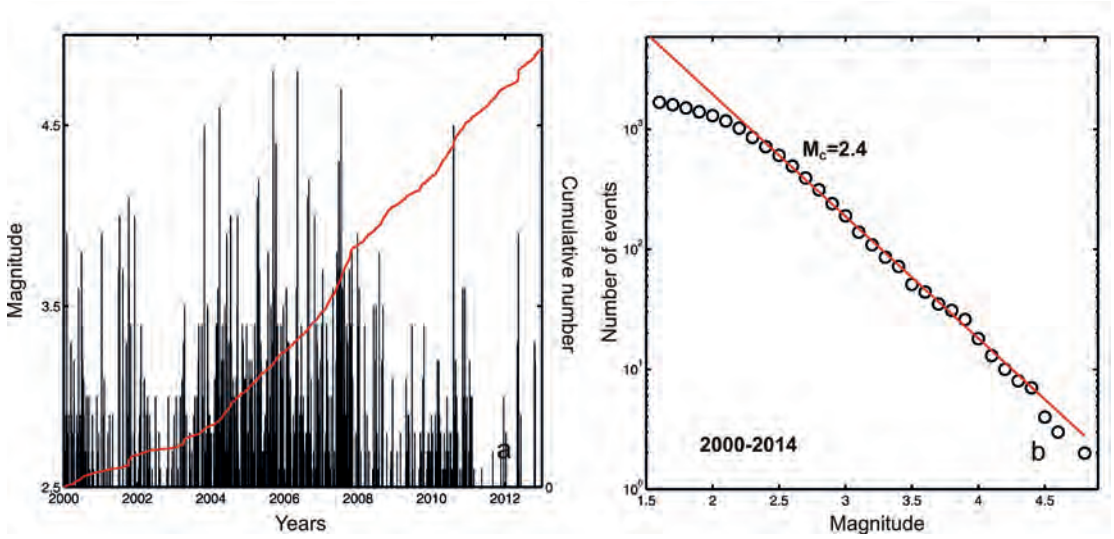

Fig. 2 - a) Comb plot for earthquake magnitude as a function of time (2000-2014), along with the cumulative frequency of earthquakes (red line). b) Earthquake magnitude distribution for the same time along with the linear regression which assigns the magnitude threshold for completeness equal to M_C=2.4.

1979; Soufleris and Steward, 1981; Soufleris *et al.*, 1982; Mercier *et al.*, 1983) transient local deployments were established (Hatzfeld *et al.*, 1986/87; Hatzidimitriou *et al.*, 1991; Papazachos *et al.*, 2000; Paradisopoulou *et al.*, 2004, 2006) and long term seismicity properties for the broader area were studied by Scordilis *et al.* (1989).

Fig. 2a schematically provides a sufficient temporal description of the earthquake magnitudes for the period 2000-2014. It seems that the low seismicity rate, the absence of strong seismicity and the restricted number of moderate earthquakes are the main characteristics of the late instrumental period. The cumulative distribution of earthquakes (red curve) signifies a small number of seismic excitations, where the slope of the curve increases abruptly. Additionally, the cumulative magnitude-frequency diagram between 2000 and 2014 (Fig. 2b) indicates the lowest threshold for magnitude completeness (M_C=2.4).

3. Data sets and relocation procedure

The accurate determination of earthquake focal parameters is strongly influenced by the crustal structure, which affects the propagation of seismic waves and consequently their recordings at the corresponding seismological stations. In an attempt to minimize the effect of crustal heterogeneity on earthquake location, local earthquake arrival times were collected from the Hellenic Seismological Network (HUSN). Network configuration guarantees the detectability of small earthquakes and an adequate number of stations with sufficient azimuthal coverage for improved relocation accuracy. Phase data were obtained from the monthly bulletins of the Seismological Station of Aristotle University of Thessaloniki (AUTh) available at http://geophysics.geo.auth.gr. Magnitudes were acquired from the monthly bulletins and they refer to M_L magnitude obtained by applying the methodology of Hutton and Boore (1987) on

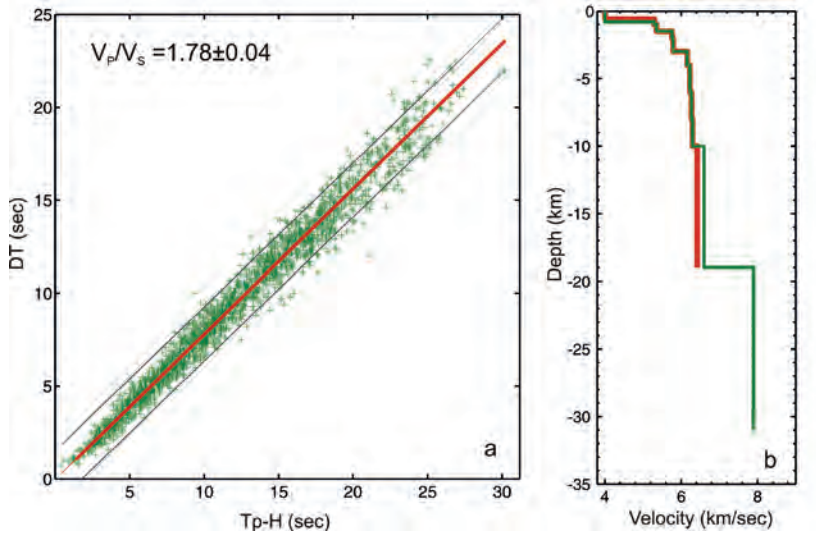

Fig. 3 - a) Cumulative Wadati diagram, indicating a linear fit (red line) between pairs of DT and T_P-H for the optimized data set of earthquakes. Grey lines show the 95% standard deviation from the mean value, V_P/V_S=1.78, b) The modified velocity model (green line), used in the current study in comparison with the velocity model adopted from Paradisopoulou *et al*. (2006) (red line).

simulated Wood Anderson earthquake recordings. In total 2288 events were collected between January 2008 and June 2014 with magnitudes 1.0≤*M*≤4.8.

For the application of the Wadati technique and the calculation of station time delays, only the most sufficient and good quality earthquake recordings were exploited. Therefore, a data set with a number of 171 earthquakes, was compiled. For each event, a satisfying number of phases (n≥7) was available, preferably recorded by 20 seismological stations in a relatively short epicentral distance (<200 km) and in adequate azimuthal coverage (stations comprised inside the circle of Fig. 1c). Considering the pairs of P- and S-wave arrivals of the constrained earthquake data set, a cumulative Wadati diagram was constructed [method introduced by Chatelain (1978)]. The time difference $DT=T_S - T_P$ between the arrival time of P-waves (T_P) and S-waves (T_S) is plotted against (T_P) for all available pairs of observations (Fig. 3a). Earthquake relocation processes presuppose the adoption of a velocity model that best approximates the structure of the Earth's seismogenic crust. Considering the local velocity models derived from microseismicity analysis (Hatzfeld *et al*., 1986/87; Papazachos *et al*., 2000; Paradisopoulou *et al*., 2006) the one that fits our data best is the one of Paradisopoulou *et al*. (2006) which was further modified for the half space, so as to incorporate longer epicentral distances, according to the crust model proposed by Panagiotopulos and Papazachos (1985) (Fig. 3b).

There is an evident linear fit, between these values, mostly accurate for pairs of smaller or intermediate distances with a mean slope equal to the velocity ratio, V_P/V_S=1.78±0.04. This value seems to be slightly larger than the ones obtained from similar studies in the same area, such as 1.74 (Hatzfeld *et al*., 1986/87) or 1.76 (Paradisopoulou *et al*., 2006). The fluctuations in the velocity ratio, is of minor importance and can be justified by the fact that local experiments used shorter epicentral distances compared to the permanent network. The spatial investigation of V_P/V_S indicated no significant distribution within the graben, also implying the absence of strong crustal variations within the brittle crust.

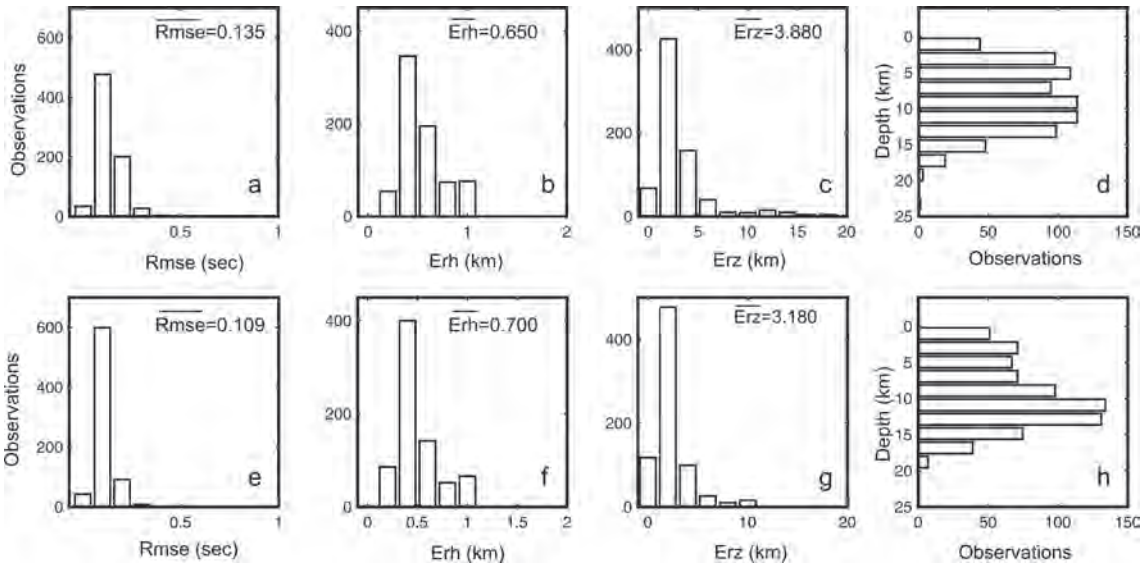

Fig. 4 - Histograms for earthquakes preliminary location (first row) and final relocation process for (second row). The mean values are given in each plot. a) root-mean square error (RMS), b) horizontal error (ERH), c) vertical error (ERZ), d) depth distribution for the preliminary results, e) root-mean square (RMS), f) horizontal error (ERH), g) vertical error (ERZ), h) depth distribution for the final results.

The travel times of seismic waves depend on the spatial and the azimuthal coverage of the seismological stations around the earthquake epicentres. New origin times for the optimal data set, have been obtained for both short and long distant seismological stations. Obtaining new origin times lies to the fact that they are deprived of uncertainties regarding the velocity model [methodology also followed by Akyol *et al.* (2006) and Karakostas *et al.* (2012)]. Therefore, the time difference between the observed and the theoretical travel times is used as a time correction for each station, a repeated procedure performed until the difference between the observed and the theoretical times becomes very small. There is a total number of 57 stations for which time residuals were estimated. The obtained corrections for the model approximately vary between -0.5 s and +0.5 s for the optimum set of data.

After the approximation of the crustal model and the station corrections, the relocation of the 2288 events was performed with the use of the Hypoinverse algorithm (Klein, 2002). Results for preliminary and final locations of the optimum set of earthquakes were compared to each other, in terms of quality parameters. So, histograms for the error in origin time (RMSE: Figs. 4a, 4e), the mean horizontal error (ERH: Figs. 4b, 4f) and the mean vertical error (ERZ: Figs. 4c, 4g) in earthquake coordinates were constructed in both cases. Although calculated errors bear only a mathematical meaning, error histograms evidence the change in the location accuracy. There is an indication of an important improvement after the incorporation of station delays in the relocation algorithm, since almost all uncertainties have been improved. An insight to the depth distribution of the relocated earthquakes is provided in Fig. 4, where the depth distribution for the final results has been shifted to 12-14 km (Fig. 4h) compared to the preliminary results (Fig. 4d) and the number of very shallow events has decreased. The depth histogram indicates the average depth of the seismogenic layer around 12-14 km. Following, relocated earthquakes estimated by the hypoinverse algorithm were further used as an input

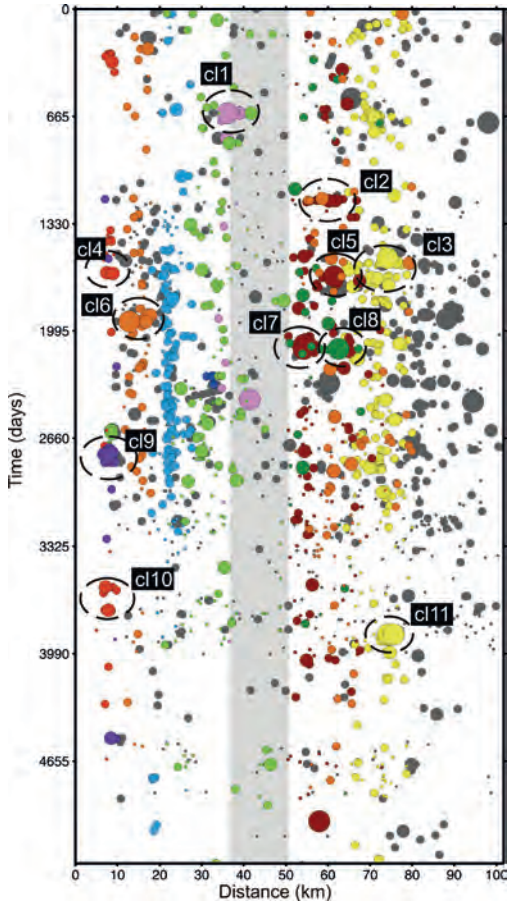

Fig. 5 - A spatial-temporal evolution plot along an E-W direction vertical plane, for the time period: 2000-2014. Different colors correspond to earthquake clusters (map view, Fig. 6), Characteristic clusters and earthquakes are highlighted. The grey zone stands for the epicentral area of the 1978 eathquakes sequence.

to HypoDD double difference algorithm (Waldhauser and Ellsworth, 2000; Waldhauser, 2001) a relative relocation program which was used in order to testify the improvement in the epicentral location and foci determination for those earthquakes which are strongly related in time and space.

4. Temporal and spatial earthquake analysis

4.1. Temporal analysis of seismicity

A temporal and spatial analysis was further performed for the recognition of microseismicity characteristics. For this reason, a space-time plot was constructed where all relocated earthquakes are projected onto a vertical 100 km long plane trending in an E-W direction (40.55°N, 22.80°E - 40.55°N, 23.90°E) which coincides with the average strike of the active TGFZ (Fig. 5). Time is converted into Julian days, starting from the beginning of 2000 and earthquake magnitude is proportional to the size of the corresponding circles. Different

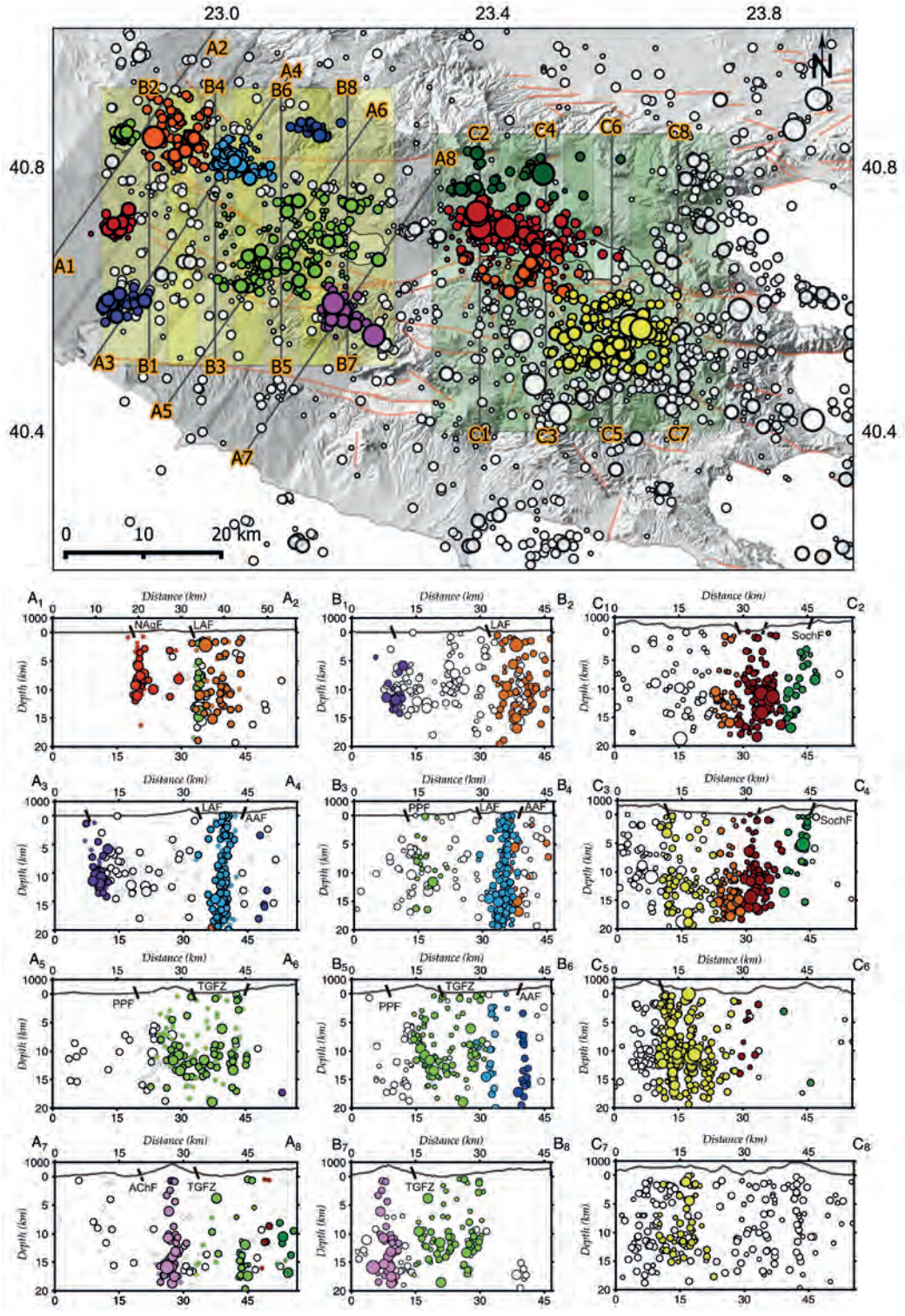

Fig. 6 - Map with the final relocated earthquake epicentres for 2000-2014. Black lines correspond to earthquake profiles displayed below. Cross-sections in a N-S direction along Lagadas area (A_1A_2, A_3A_4, A_5A_6, A_7A_8), in a NE-SW direction along Lagadas area (B_1B_2, B_3B_4, B_5B_6, B_7B_8) and in N-S direction over Arnea and Volvi sub area (C_1C_2, C_3C_4, C_5C_6, C_7C_8) along with the corresponding geomorphological profiles. Colors for earthquake foci are the same in the map view and the profiles.

colors correspond to subareas with specific geographic coordinates. The existence of discrete prolonged earthquake bands is clearly evidenced. From east to west, parallel stripes of earthquake activity reveal a constant occurrence of events around Lagadas Lake, Volvi Lake and Arnea area. However, there is a characteristic band which mediates between Lagadas and Volvi Lake with scarce seismicity (background grey zone, at approximately 45 km from the beginning of the profile) around the epicentral area of the 1978 event. In the beginning of 2001, a seismic swarm with two events of magnitudes 4.5 and 4.1 (October 8, 2001, with a thirty minutes lag), occurred in Chortiatis Mountain (cl1, pink color) and lasted for some days. Two more isolated events of magnitude *M*=4.0 occurred at the eastern part of Arnea in the same year, not followed by seismic activity. In April 2003 a small excitation with maximum magnitude *M*=3.3 (cl2, red color) and a short duration occurred at the northern boundary of Volvi Lake. No other moderate events occurred until 2004, whereas during 2004-2005 seismic activity increased. The time interval 2004 to 2008 (Julian days: 1300-3200) comprises a time-window where seismicity rate is higher and it coincides with a seismic burst at the western part of the study area. A seismic excitation initiated (cl4, red color) and some years later another group of events followed (cl10, red color).

Additionally, in 2005 two adjacent clusters started simultaneously (earthquakes in blue and orange color, at 20 km and 18 km respectively, from the beginning of the plot), showing a constant interaction of seismicity for some years. Especially in 2005, a seismic excitation (cl6, orange color) culminated in an earthquake with magnitude equal to 4.2 (April 2005). There is a simultaneous seismic activity (light blue color) in progress north of Lagadas Lake, where there is no recorded event stronger than 3.1. At the termination of LAV fault there is a swarm of events (red color, which are found at approximately 8 km from the start of the section). It is noticed that there is a sequence of short seismic excitations situated at the northern margin of Volvi, (cl5, red color) and a subsequent concentration in Arnea (cl3, yellow color). In 2005 there is seismic activity at the northern part of Volvi Lake (cl7, dark red color - cl8, green color) and at the western termination of SochF with a number of moderate events ranging from 4.0 to 4.8. In 2007 a seismic excitation occurred in Thermaikos Gulf (cl9, purple color) with a maximum magnitude *M*=4.4. In 2010 a couple of events (*M*=4.4, *M*=4.5) occurred around Arnea followed by a small number of aftershocks (cl8, green color). The last moderate event for the time of the observations took place in October 2013 and concerns a *M*=4.4 event at the northern boundary of Volvi Lake, not followed by minor magnitude earthquakes.

4.2. Spatial analysis of seismicity

As evidenced in the temporal analysis, seismicity is not evenly distributed in the entire area. Fig. 6 illustrates the characteristic spatial patches of earthquakes and in the majority of the cases they are localized along the E-W and NW-SE rupture zones at the NW, the central and the west part of the study area. Hence, the majority of the epicentres are located at the western and the eastern part of the TGFZ and to the broader area of Arnea and Poligiros. On the other hand, there is nearly an absence of seismicity along seismogenic faults, such as AnF and StF zones, both associated with the strong historical events in 1677 (*M*=6.2) and 1932 (*M*=7.0) respectively. A lack of seismicity is evident, in the central part of the TGFZ where 1978 earthquakes occurred, with the exception of the 2013 minor magnitude seismic excitation with maximum magnitude *M*=3.3. For the accurate investigation of the foci distribution and

their relevance to the geometry of the structures, twelve successive cross-sections perpendicular or semi perpendicular to the main structures are constructed in accordance to the least principal stress axis (Fig. 6). In particular SW-NE sections A_1A_2, A_3A_4, A_5A_6 and A_7A_8 are developed perpendicularly to the general strike of the NE-SW fault segments that bound the Lagadas sub basin. N-S profiles (B_1B_2, B_3B_4, B_5B_6 and B_7B_8) are normal to the active TGFZ segments, four additional N-S trending profiles (C_1C_2, C_3C_4, C_5C_6 and C_7C_8) are normal to the E-W faults which extend towards the eastern part of the study area. Sections B_1B_2, B_3B_4, B_5B_6 are not the most representative for the NW-SE trending faults but they are suitable for the foci investigation of the E-W trending faults. In all cases, cross-sections include epicentres in the range of 5 km in width alongside each profile, from south to north. Colors are found in correspondence with the ones of Fig. 5. In A_1A_2 and B_1B_2 sections, earthquakes which belong to the clusters cl4, cl6, cl9, c10 are projected. Cl4 and cl10 earthquake clusters form a plane dipping at a high angle up to 10 km in depth. The fault plane solution of the strongest event is associated with a fault that dips approximately 50° to the SW. This dip agrees with the fault plane solutions calculated by Paradisopoulou *et al.* (2004) and can be associated with Nea Aghialos fault (NAgF) (Tranos *et al.*, 2003). No important seismicity in this area is available so as to acquire further information about this seismogenic zone. A cluster of green epicentres is found at the termination of LAVF system with a very steep dip. At A_3A_4 and B_3B_4 cross sections foci distribution of the blue colored earthquakes is forming seismogenic zones dipping steeply (more than 70°) to the south at depths up to 20 km. Sections A_5A_6 and B_5B_6 crosses the PPFS to the south and the SochF to the north. A group of small events is also visible, northern than SochF where a small fault activated for 6 days (blue color). It is not clear to distinguish if the foci met in the centre of Lagadas correspond to an activation of AAF segment or SochF. However, it is characteristic that they follow a NW-SE trend. The cl1 cluster around the mountain of Chortiatis is visible in sections A_7A_8 and B_7B_8. Hypocentral depths are distributed from 10 to 18 km and the available fault plane solutions from Paradisopoulou *et al.* (2006) indicate a fault at 114° strike dipping to the north at about 50°. There is no other seismic burst in this area apart from the 2001 cluster of events. Following, section B_7B_8 is more representative than the corresponding NW-SE one, for the examination of AChF system, where two southdipping and northdipping fault planes are defined.

Earthquake profiles that extend to the western part are normal to the E-W fault zones, where the main active normal SochF and NApF dominate. Volvi region is seismically active in longer zones, since there are numerous earthquakes distributed along the basin boundaries. Fault plane dips around Volvi boundaries are very well defined. Foci distribution of clusters cl2, cl5, cl7 and cl8 are projected onto the cross sections C_1C_2 and C_3C_4 that are normal to the main rupture zones. The foci distribution is well defined and lies in total accordance with the geological data. Foci to the north dip at high angles to the south (60°), and are strongly associated with SochF (C_1C_2, C_3C_4). However seismicity in sections C_5C_6 and C_7C_8, there is an activation of subsidiary faults with different orientations and the seismicity pattern seems to be more diffuse rather that distributed around known important faults.

Specific clusters of events were further relocated with the help of the advanced HypoDD algorithm. The number of the relocated events is smaller since events which are not strongly correlated are removed as outliers. Therefore, relocated earthquakes are more densely distributed and show a stronger degree of clustering. For this reason, the area was further subdivided into distinct subsets of data, displayed in rectangular areas of Fig. 7, where the

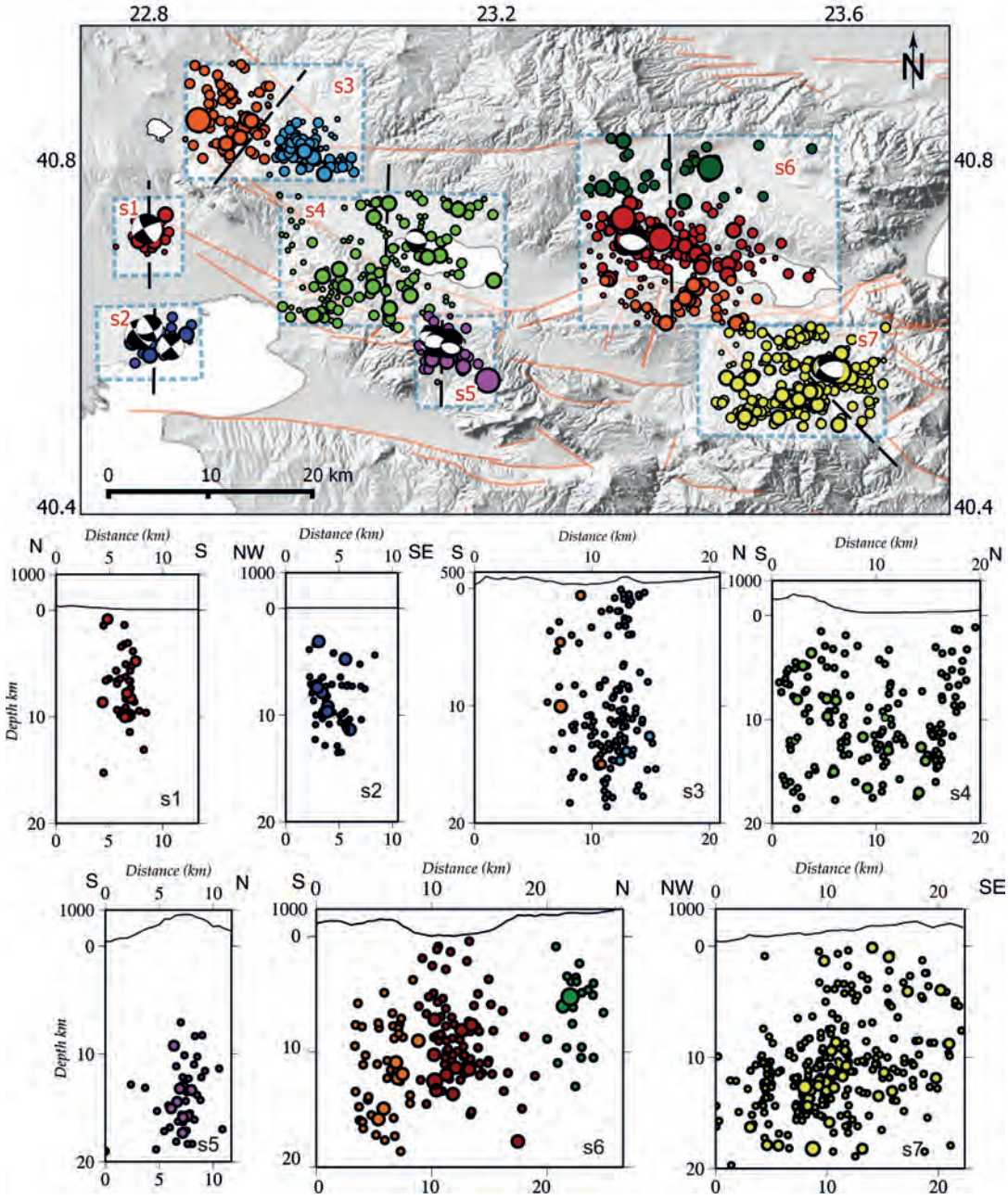

Fig. 7 - Map with the areas where the relative relocation with the HypoDD algorithm was applied. Cross-sections of the relocated foci (after HypoDD) with the corresponding geomorphological profiles. Available fault plane solutions are also used.

relocated seismicity is characterized by the lowest possible uncertainties. For the identification of the active segments comprising the active fault population, available fault plane solutions have been employed by previous research (Paradisopoulou *et al.*, 2006; and the catalogue of the seismological station of Thessaloniki, http://geophysics.geo.auth.gr/ss/).

The relocation for clusters enclosed in s1 and s2 subsets agree with the results provided by Hypoinverse algorithm. The range of earthquake depths in s1 form a rupture zone reaching the depth of 11 km, dipping to the SW. The same depth range is noticed in s2 subset, where the responsible fault is probably dipping to the SE. In s3 rectangle, two seismic clusters are visible. Considering the cross-section s4, foci in both cases are developing zones dipping in high angles at depth. In rectangle s4 foci distribution at depth is concentrated between 5-16 km around Lagadas Lake, generated by the north and south bounding faults. Two sub regions are introduced in the eastern part, around Volvi Lake. Not important differentiations are revealed from the spatial distribution of the relocated epicentres along SochF in the two cases of relocation techniques (s6). There is a visible gradual dipping of SochF to the south, whereas there is a seismic activity attributed to NApF. Subplot s7 presents the Arnea - Poligiros region and corresponds to the mountainous area southern than Volvi Lake, where seismicity seems not to be locally concentrated around major faults but it is dispersed around the fault network. However there is an indication of dipping of structure zones dipping at 45° to the north.

5. Discussion

Small magnitude earthquakes reveal a spatial-temporal clustering and a migration mechanism, which can be served as a tool to constrain geometric and kinematic properties at the activated structures (fault segments or fault systems). In our case, long term seismicity in Mygdonia basin between 2000 and 2014 was relocated in an attempt to unveil properties of the associated fault population. The incorporation of the best well-fitted velocity model, the calculation of station time delays and the velocity ratio derived from the data used, individually contributed to an important improvement in the precision of earthquake coordinates. The striking observation extracted from the analysis is that Mygdonian seismicity is not evenly distributed in the entire area but occurs along deformation zones in space and time, at both margins of the graben. Diffuse off-fault seismicity is also evident especially around Arnea and Poligiros where isolated moderate events occur. Major active zones, although having the potential, are lacking seismicity, such as the epicentral area of the 1978 earthquake, probably attributed to stress re-distribution (Tranos *et al.*, 2003) and moderate slip rates of 1mm/yr (Kotzev *et al.*, 2001). On the other hand, Arnea region, as a direct consequence of stress increase after the 1978 event, shows a constant occurrence of minor earthquakes, with magnitudes $M \leq 4.8$. Our perception about the width of the brittle crust and the dips of the active faults was enhanced by investigating the hypocentral distribution with the use of successive profiles. The width of the seismogenic zone is confined between 5 and 18 km. Seismogenic structures, especially the ones which are strongly influenced from the previous seismotectonic episodes comprise inherited structures with low seismicity and fault planes with high dipping angles, almost vertical. The complex seismotectonic episodes along with the clockwise rotation of the region have imposed their effects on the structures (Kissel *et al.*, 1985; Pavlides *et al.*, 1988). A considerable amount of earthquakes is generated along NW-SE sub-basin bounded from AAF and LAVF zone, with the indications that boundaries are seismogenic. Evidence is not very clear for the antithetic LAvF, however it seems that there is a number of earthquakes associated with this fault segment. In the case of the seismic activation of AAF, it is visible

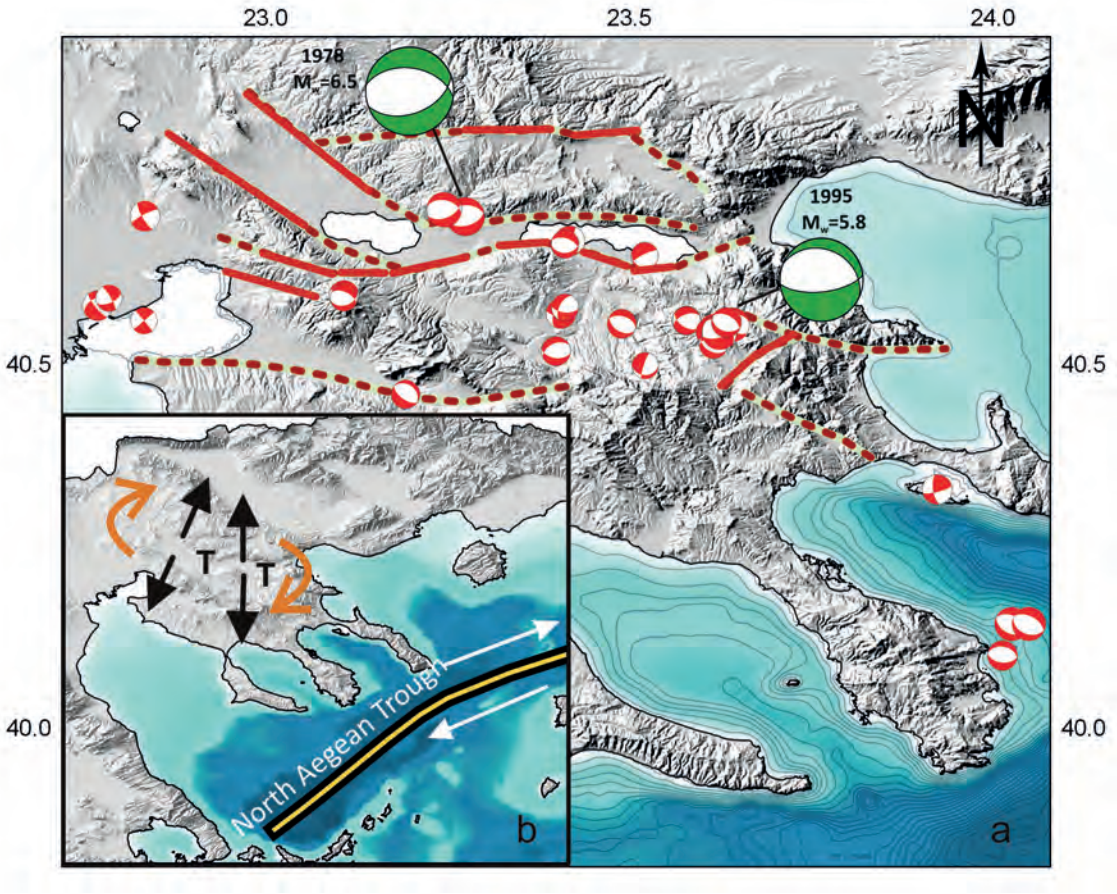

Fig. 8 - a) Simplified map which summarizes the main active seismotectonic zones of Mygdonia region in the extensional region of northern Greece which are under the additional influence of the North Anatolian Fault. Fault plane solutions of the two strongest recent earthquakes of Thessaloniki and Arnea which verify the orientation of the current stress field. The main active segments of the fault population which were seismogenic during the years of observations are marked by red color. b) The same area with the main kinematics which impose their impact on the seismogenic faults and earthquake occurrence.

that epicentres are located at the conjunction of SochF and AAF, implying that a possible propagation of SochF to the west, which is probably causing the activation of AAF, whose general strike is not oriented in accordance to the least principle stress axis. The foci distribution of apparent E-W structures show dips around 50°. Clusters associated with SochF show a steep dip fault plane, in accordance with the geometry of the surface fault trace. The structure of SochF at depth was not revealed before. The cascade of moderate events at the northern margin of Volvi shows that there is an interaction of the north and south-dipping faults at this part of the graben. The possible propagation of high-angle dipping SochF in the north, which diminishes to the west, affects the seismic activity close to Assiros. The foci planes dip with approximately 70°- 80° to the SW. This agrees with the suggestion of Pavlides and Kilias (1987), who affirmed that especially the south dipping faults are related to high angles normal faults. On the other hand, as far as Volvi area is concerned, it can be deduced that the seismicity pattern is localized and there is a constant migration of seismic activity between different clusters of earthquakes,

whereas it is more distributed in the southern part of the area, around Arnea village, where a SW-NE structure zone is activated. It is evident that, contrary to the general statement of Goldsworthy *et al*. (2002), there is an additional south dipping activity in Mygdonia graben. Moderate seismic excitations are attributed to SochF with foci reaching 17 km in depth, whose fault plane is well defined. The southern zones (NApF) are also seismogenic, exhibiting lower dips. Aspects expressed by previous research based on limited local network data are now confirmed by a long-term seismicity observation.

Finally, the faults that were favourable to slip and belong to the active fault population of the area deduced from this study are the ones presented in Fig. 8. Additional data, regarding fault plane solutions derived from local experiments, after the 1978 earthquake are shown. The deformation zones are also shown in Fig. 8, where N-S extension dominates at the western part of the region, however, at the eastern part, NE-SW extension is measured because of the reactivation of the NW-SE faults that have been anti-clockwise rotated.

The stress field in Mygdonia graben shows a general N-S extension, exhibiting a spatial variation of the least stress axis orientation from NNW-SSE to NNE-SSW which also agrees with the "S-shaped" basin formation (Mountrakis *et al*., 2006; Vamvakaris *et al*., 2006). The widespread extension has been measured by different studies, however, in every case, the fault plane solutions totally agree with the foci distribution and the geometry of the active faults. However, the barrier raised for the clear determination of fault seismogenesis is connected with the fact that the fault network is composed by a synthesis of small faults whose strike is locally aligned with the stress tensor. It seems that in Lagadas area seismicity is adjusted to the coexistence of two characteristic sets of faults that accommodate stress.

Although, there is a decay of strong seismicity rate during the last years, taking into consideration all available data, behavior of Mygdonia seismicity suggests a successive migration between adjacent segments of TGFZ both to the east and the west. The investigation of background seismicity is underlined in this study since results provide an important contribution to the study of fault interaction at depth, seismotectonic zoning in areas where background seismicity is an important process. This approach reveals additional information on the development of the seismogenic structures deprived of clear surface trace, that exist within an active seismotectonic environment such as the seismically active grabens that are met in Greece.

Acknowledgments. We are grateful to the editorial assistance of L. Hutchings as well as the two anonymous reviewers for their creative comments. This research was co-financed by the European Union (European Social Fund-ESF) and Greek national funds through the Operational Program "Education and Lifelong Learning" of the National Strategic Reference Framework (NSRF) - Research Funding Program: Heracleitus II Investing in knowledge society through the European Social Fund. Plots were made using the Generic Mapping Tools version 4.5.3 (www.soest.hawaii.edu/gmt, Wessel and Smith, 1995) and the QGIS Geographic Information System, Open Source Geospatial Foundation Project (http://qgis.osgeo.org). Department of Geophysics, Aristotle University of Thessaloniki, contribution number 824.

REFERENCES

Akyol N., Zhu L., Mitchel J., Sözbilir H. and Kekovali K.; 2006: *Crustal structure and local seismicity in Western Anatolia*. Geophys. J. Int., **166**, 1259-1269.

Bagh S., Chiaraluce L., De Gori P., Moretti M., Govoni A., Chiarabba C., Di Bartolomeo P. and Romanelli M.; 2007*: Background seismicity in the central Apennines of Italy: the Abruzzo region case study*. Tectonophys., **444**, 80-92.

Chatelain J.; 1978: *Etude fine de la sismicité en zone de collision continentale à l'aide d'un réseau de stations portables: la région Hindu-Kush-Pamir.* Ph.D. thesis, Univ. Paul Sabatier, Toulouse, France.

Goldsworthy M., Jackson J. and Haines J.; 2002: *The continuity of active fault systems in Greece*. Geophys. J. Int., **148**, 596-618.

Hatzfeld D., Christodoulou A., Scordilis E., Panagiotopoulos D. and Hatzidimitriou M.; 1986/87: *A microearthquake study of the Mygdonian graben (northern Greece)*. Earth Planet. Sc. Lett., **81**, 379-396.

Hatzidimitriou P., Hatzfeld D., Scordilis E., Papadimitriou E. and Christodoulou A.; 1991: *Seismotectonic evidence of an active normal fault beneath Thessaloniki (Greece)*. Terra Motae, **3**, 648-654.

Hutton L. and Boore D.; 1987: *The M scale in southern California*. Bull. Seismol. Soc. Am., **77**, 2074-2094.

Karakostas V., Karagianni E. and Paradisopoulou P.; 2012: *Space-time analysis, faulting and triggering of the 2010 earthquake doublet in western Corinth gulf*. Nat. Hazards, **63**, 1181-1202.

Kissel C., Laj C. and Muller C.; 1985: *Tertiary geodynamical evolution of northwestern Greece: paleomagnetic results*. Earth Planet. Sci. Lett., **72**, 190-204.

Klein F.; 2002: *User's Guide to HYPOINVERSE-2000, a Fortran program to solve earthquake locations and magnitudes*. U.S. Geol. Surv., Open File Report 02–171, Version 1.0, Menlo Park, CA, USA, 117 pp.

Kotzev V., Nakov R., Georgiev T., Burchfiel B. and King R.; 2001: *Crustal motion and strain accumulation in western Bulgaria*. Tectonophys., **413**, 189-200.

Maggi C., Frepoli A., Cimini G., Console R. and Chiappini M.; 2009: *Recent seismicity and crustal stress field in the Lucanian Apennines and surroundings areas (Southern Italy): seismotectonic implications*. Tectonophys., **463**, 130-144.

McKenzie D.; 1978: *Active tectonics of the Alpine-Himalayan belt: the Aegean Sea and surrounding regions*. Geophys. J. R. Astron. Soc., **55**, 217-254.

Mercier J., Carey-Gailhardis E., Mouyaris N., Simeakis K., Roundoyannis T. and Anghelidhis C.; 1983: *Structural analysis of recent and active faults and regional state of stress in the epicentral area of the 1978 Thessaloniki earthquakes (northern Greece)*. Tectonics, **2**, 577-600.

Mountrakis D., Tranos M., Papazachos C., Thomaidou E., Karagianni E. and Vamvakaris D.; 2006: *Neotectonic and seismological data concerning major active faults and the stress regimes of Northern Greece*. Geol. Soc., London, Special Publications, **260**, 649-670, doi:10.1144/GSL.SP.2006.260.01.28.

Panagiotopulos D. and Papazachos B.; 1985: *Travel times of Pn waves in the Aegean and surrounding area*. Geophys. J. R. Astron. Soc., **80**, 165-176.

Papazachos B. and Comninakis P.; 1971: *Geophysical and tectonic features of the Aegean arc*. J. Geophys. Res., **76**, 8517-8533.

Papazachos B. and Papazachou C.; 2003: *The earthquakes of Greece*. Ziti Publication, Thessaloniki, Greece, 304 pp.

Papazachos B., Mountrakis D., Psilovikos A. and Leventakis G.; 1979: *Surface fault traces and fault plane solutions of the May-June 1978 major shocks in the Thessaloniki area, Greece*. Tectonophys., **53**, 171-183.

Papazachos C., Soupios P., Savvaidis A. and Roumelioti Z.; 2000*: Identification of small-scale active faults near metropolitan areas: an example from the Asvestochori fault near Thessaloniki*. In: Proc. XXXII ESC General Assembly, Lisbon, Portugal, pp. 221-225.

Paradisopoulou P., Karakostas V., Papadimitriou E., Tranos M., Papazachos C. and Karakaisis G.; 2004: *Microearthquake study of the broader Thessaloniki area*. In: Proc. 5th Int. Symp. Eastern Mediterranean Geol., Thessaloniki, Greece, vol. 2, pp. 623-626.

Paradisopoulou P., Karakostas V., Papadimitriou E., Tranos T., Papazachos C. and Karakaisis G.; 2006: *Microearthquake study of the broader Thessaloniki area (Northern Greece)*. Ann. Geophys., **49**, 1081-1093.

Pavlides S. and Kilias A.; 1987: *Neotectonic and active faults along the Serbomacedonian zone (SE Chalkidiki, northern Greece)*. Ann. Tectonicae, **1**, 97-104.

Pavlides S., Kondopoulou D., Kilias A. and Westphal M.; 1988: *Complex rotational deformations in the Serbo-Macedonian massif (north Greece): structural and paleomagnetic evidence*. Tectonophys., **145**, 329-335.

Scordilis E., Karakaisis G., Papadimitriou E. and Margaris B.; 1989: *Microseismicity study of the Servomacedonian zone and the surrounding area*. Geol. Rhodopica, **1**, 79-83.

Soufleris C. and Steward G.; 1981: *A source study of the Thessaloniki (northern Greece) 1978 earthquake sequence*. Geophys. J. R. Astron. Soc., **67**, 343-358.

Soufleris C., Jackson J., King G., Spencer C. and Scholz C.; 1982: *The 1978 earthquake sequence near Thessaloniki (northern Greece)*. Geophys. J. R. Astron. Soc., **68**, 429-458.

Tan O.; 2012: *The dense micro-earthquake activity at the boundary between the Anatolian and South Aegean microplates*. J. Geodyn., **65**, 199-217.

Tranos M., Papadimitriou E. and Kilias A.; 2003: *Thessaloniki-Gerakarou fault zone (TGFZ): the western extension of the 1978 Thessaloniki earthquake fault (northern Greece) and seismic hazard assessment*. J. Struct. Geol., **25**, 2109-2123.

Vamvakaris D., Papazachos C., Karagianni E., Scordilis E. and Hatzidimitriou P.; 2006: *Small-scale spatial variation of the stress field in the back-arc Aegean area: results from the seismotectonic study of the broader area of Mygdonia basin (N. Greece)*. Tectonophys., **417**, 249-267.

Waldhauser F.; 2001: *HypoDD: a computer program to compute double-difference hypocenter locations*. U.S. Geol. Surv., Open File Report 01-113, Menlo Park, CA, USA, 25 pp.

Waldhauser F. and Ellsworth W.L.; 2000: *A double-difference earthquake location algorithm: method and application to the Northern Hayward Fault, California*. Bull. Seismol. Soc. Am., **90**, 1353-1368.

Wessel P. and Smith W.H.F.; 1995: *New version of the generic mapping tools*. Eos Trans. AGU, **76**, 329-336, doi:10.1029/95EO00198.

Corresponding author: Charikleia Gkarlaouni
Geophysics Dpt., School of Geology, Aristotle University
Address GR-54 124, Thessaloniki, Greece
Phone: +30 2310 998488; fax: +30 2310 998528; e-mail: hagarl@geo.auth.gr